Journal of Molecular Liquids 333 (2021) 115932

Contents lists available at ScienceDirect

Journal of Molecular Liquids

journal homepage: www.elsevier.com/locate/molliq

Performance assessment of five adsorbents based on fly ash for removal of cadmium ions

Gabriela Buema [a], Nicoleta Lupu [a], Horia Chiriac [a], Gabriela Ciobanu [b], Roxana-Dana Bucur [c,*], Daniel Bucur [c], Lidia Favier [d], Maria Harja [b,*]

[a] National Institute of Research and Development for Technical Physics, 47 Mangeron Boulevard, Iasi, Romania
[b] "Gheorghe Asachi" Technical University of Iasi, Faculty of Chemical Engineering and Environmental Protection, 73 Prof. dr. docent Dimitrie Mangeron Str., 700050, Iasi, Romania
[c] University of Agricultural Sciences and Veterinary Medicine Iasi, Romania
[d] Univ Rennes, Ecole Nationale Supérieure de Chimie de Rennes, CNRS, ISCR – UMR6226, F-35000 Rennes, France

ARTICLE INFO

Article history:
Received 5 February 2021
Received in revised form 8 March 2021
Accepted 14 March 2021
Available online 18 March 2021

Keywords:
Cadmium ion adsorption
Fly ash
Kinetic models
NaOH treatment
Zeolites

ABSTRACT

Five adsorbents based on fly ash treated with NaOH for the adsorption of cadmium ion from aqueous solutions were investigated. The materials were characterized using scanning electron microscopy (SEM), Fourier transform infrared spectroscopy (FTIR) and the Brunauer-Emmett-Teller (BET) surface area methods. The results demonstrated that the specific surface area of fly ash was improved after NaOH treatment, and that the adsorption of cadmium by the new adsorbents reached equilibrium in less than 120 min. The results also confirmed that the materials treated with NaOH solution by direct activation had a higher adsorption capacity than untreated fly ash. The maximum adsorption capacities obtained were in the range of 9.18–48.5 mg/g. Also, SEM/EDS and FT-IR results of Cd(II) loaded adsorbents were performed. The obtained experimental data were used for kinetics determination using three model equations: a pseudo first-order model, a pseudo second-order model, and the intraparticle diffusion model. Was found that the adsorption of cadmium ions onto the adsorbents studied follows the pseudo second-order model. The adsorption isotherms of the adsorbent synthesized by direct activation for 15 h using 5 M NaOH at 90 °C with a ratio of 1:3 fly ash: NaOH (A5) was assessed in terms of the Langmuir (four types of linearization), Freundlich, Temkin, Harkin-Jura, and Halsey models. The effectiveness of the adsorbents was evaluated using the toxicity characteristic leaching (TCLP) procedure. Accordingly, the proposed methods in this study are recommended for advanced capitalization of fly ash, particularly as a potential adsorbent for the removal of cadmium ions from wastewater.

1. Introduction

The contamination of water with various pollutants is a serious problem in the area of environmental protection that needs to be solved [1,2]. Improving the adsorption efficiency of heavy metal ions onto eco-friendly adsorbents has become an important matter in the sustainable use of wastes [3,4]. Adsorption onto different solids eliminates heavy metals from the wastewater, thus reducing its toxicity. A variety of materials such as activated carbon, commercial zeolites, mesoporous material, and clay are widely used as an adsorbent, but these materials are expensive [5,6]. The possibility of producing low cost absorbents that can be applied to water depollution has been investigated in recent years [7–9].

The demand for energy has increased over time, and of the various sources of energy, coal remains one of the most widely utilized [10,11]. Approximately 25% of the global primary energy required is supplied by coal [12]. Coal burning in power stations results in around 750 million tons of ash annually, of which less than 25% has been utilized. Iron and calcium oxides, sulphate and trace elements such as arsenic, manganese, cadmium, chromium, lead, selenium, and vanadium are the major impurities in fly ash [13].

There are various opportunities for capitalizing on the fly ash by-product, according to its chemical and technological properties [10], including: in ceramics [14], in geopolymers [15,16], in the agricultural sector [17], for adsorption [18,19], in catalysis [2], and as zeolites [20,21]. Fly ash is a pozzolanic mixture resulting from the combustion of coal at temperatures between 650 and 800 °C [15,22,23]. In order to reduce the problems caused by its storage, fly ash has been intensively investigated as a starting material in different fields of research [24–30]. Among these fields, the modification of fly ash with an alkaline reagent using methods such as direct activation, fusion, ultrasound, and

* Corresponding author.
E-mail addresses: gbuema@phys-iasi.ro, nicole@phys-iasi.ro (G. Buema), hchiriac@phys-iasi.ro (H. Chiriac), gciobanu@tuiasi.ro (G. Ciobanu), rdbucur@uaiasi.ro (R.-D. Bucur), dbucur@uaiasi.ro (D. Bucur), lidia.favier@ensc-rennes.fr (L. Favier), mharja@tuiasi.ro (M. Harja).

https://doi.org/10.1016/j.molliq.2021.115932
0167-7322/

microwaves has been proposed as one way to solve the storage problem [17,27,31–33].

Many adsorbents have been tested for the removal of Cd (II) ions from wastewater, and adsorbents based on fly ash have been proposed due to their potential to increase adsorption capacity [25,30,34], given that they have a high surface area, are easy to synthesize, and are cost effective. These new materials present characteristic peaks corresponding to quartz, mullite, sodalite, hematite, chabazite, hydroxysodalite, gismodine, Na—Y, Na—P1, and faujasite, which are of special interest [7,35]. Sources of water pollution containing Cd (II) ions include the metallurgy, steel, petrochemical, textile, extractive, inorganic and organic chemical industries [25,36]. The classical techniques for Cd (II) ion elimination from wastewaters (ion-exchange, solvent extraction, chemical precipitation, phytoextraction, ultrafiltration, reverse osmosis, electrodialysis) are costly and require high energy consumption [37]. Additionally, the adsorption process is one of the most effective processes for reducing Cd (II) ions in effluents. We have previously reported results regarding the adsorption of Cd (II) ions by a new material obtained by treating fly ash with sulphuric acid [8].

The current study was conducted with the aim of developing promising low cost adsorbents by treatment of fly ash with NaOH and confirming their adsorption properties for Cd (II) removal. The adsorption of cadmium ions was chosen for investigation due to their negative effects on the environment and human health. The Cd (II) adsorption behavior of fly ash in comparison with six new materials obtained by treatment of fly ash with NaOH using the direct activation method (ultrasound method) was assessed. In the first part of the study, the effect of contact time was investigated in batch adsorption experiments. The experimental data obtained from this study were completed by analyzing the adsorption isotherms. In the second part of the study, the data on cadmium adsorption by the adsorbents were matched to the Langmuir (four types of linearization), Freundlich, Temkin, Harkin-Jura, and Halsey models.

All five adsorbents based on fly ash were obtained easily, and therefore the new materials exhibited the advantage of easy synthesis. The results of this study may help establish the adsorption performance of new materials obtained using different conditions of synthesis. This study suggests an economical way to reduce the environmental problem caused by the fly ash disposal. The presented synthesis procedures by direct activation method and ultrasound method confirmed that the materials synthesized based on fly ash are cheap and can be considered the effective adsorbents for Cd(II) ions from aqueous solution.

2. Materials and methods

2.1. Adsorbent preparation and characterization

The fly ash (A0) used in this work was collected in March 2020 from the CET II Holoca (Iasi, Romania). Fly ash is grey in colour and has spherical particles and small quantities of irregular shaped particles (presence of unburned carbon) [10]. It has a specific surface area of 7.23 m^2/g, pore volume of 2.439 10^{-2} cm^3/g, mean particle diameter of 0.24 μm (R50 was 0.45 μm), loss of ignition of 7.4% and real density equal to 2248 kg/m^3, the results being similar to those of other types of fly ash [38].

All chemicals were purchased from the Chemical Company (Iasi, Romania) and they were used without any purification.

The synthesized adsorbents were characterized by SEM, FTIR and the BET surface area method as follows: the morphology was determined using SEM/EDS analysis performed using Scanning Electron Microscope SEM JEOL JSM 6390; the Scanning Electron Microscope (SEM) is equipped with Energy-Dispersive X-RAY Spectroscopy (EDS) system; Fourier Transform Infrared Spectroscopy (FT-IR) was performed on a Thermo Scientific Nicolet 6700 FT-IR spectrometer; after adsorption FTIR analysis was performed using Alpha Bruker FT-IR spectrometer, spectral range: 4000–400 cm^{-1}, and 4 cm^{-1} resolution; Nitrogen physical sorption was carried out at −196 °C on an Autosorb 1-MP gas sorption system (Quantachrome Instruments, Boynton Beach, FL, USA); a Buck Scientific spectrophotometer was used for cadmium ion detection (Buck Scientific, East Norwalk, CT, USA).

The A1–A5 materials were obtained after the treatment of A0 material with NaOH solution, using two solid:liquid ratio of 1:3, respectively 1:5. The choice of NaOH for the synthesis of materials was based on the pronounced basic character of this reagent (NaOH is a strong base, which dissociates completely in aqueous solution). Also, the literature shows a series of chemical activation agents that can be used in the synthesis of materials such as NaOH, KOH, Na_2CO_3, etc. [39,40].

The A1 material was prepared by the direct activation method as follows: briefly, a quantity of fly ash (50 g) was added to 150 mL of 2 M NaOH at room temperature. The contact time was 168 h. The A2 and A3 materials were synthesized by the ultrasound method at 70 °C with 1 h (A2) or 2 h of contact time (A3). The fly ash:NaOH ratio in both cases was 1:5. The synthesis of A4 material was carried out at 90 °C with a NaOH concentration of 5 M, corresponding to a mixture with a fly ash:NaOH ratio of 1:5. The A5 material was prepared by direct activation for 15 h by 5 M NaOH at 90 °C; the fly ash:NaOH ratio was 1:3.

All the materials obtained were cooled and crystallized for 18 h at room temperature. Finally, the materials were dried for 24 h at 60 °C and kept in a PE bag until required for the adsorption experiments. The study conditions were chosen on the basis of preliminary studies [7,17,23], in order to compare the methods based on activation at ambient temperature with activation at high temperatures, with or without ultrasound.

2.2. Adsorption, desorption and kinetic study

A stock solution of 1000 mg/L Cd (II) was prepared by dissolving a quantity of $Cd(NO_3)_2$ $4H_2O$ in deionized water. All working solutions were obtained by further dilution with deionized water. A standard calibration curve was determined previously.

All experiments were performed using the batch method, at ambient temperature with intermittent stirring. In the kinetic investigation of Cd (II) ion adsorption onto the A0–A5 materials, approximately 30 mg of each adsorbent were placed in separate vials together with 10 mL of Cd (II) solution (250 mg/L) and then the residual concentrations were analyzed at each time interval. All experiments were performed at pH 5, for a period of 120 min at room temperature. The pH value was established according to the literature [41,42]. The zero point charge pH (pH_{zpc}) of the materials synthesized from fly ashes was 3.80, so the surface has a positive charge at the pH<pH_{zpc}, as the competition between Cd (II) and H^+ on the adsorbent surface impedes the adsorption of Cd (II). Cd (II) precipitated at a pH above 7 was avoided.

The quantity of Cd (II) adsorbed (q, mg/g) was calculated using Eq. (1):

$$q, mg/g = \frac{(C_i - C_t)V}{m} \quad (1)$$

where C_i is the initial Cd (II) concentration, C_t (mg/ L) is the Cd (II) concentration at different time intervals (mg/L), V (L) is the volume of the Cd (II) solution and m (g) is the quantity of the adsorbents used.

For the adsorption study, 0.4 g of adsorbent was stirred with 50 mL of the initial Cd (II) concentration (100–350 mg/L range), at pH 5, for a period of 24 h at room temperature. The residual concentrations were analyzed for each initial concentration, by the spectrophotometric method, using xylenol orange at 575 nm wavelength, with a Buck Scientific spectrophotometer. The sample concentrations were calculated with reference to the calibration curve (previously obtained). The quantity of Cd (II) adsorbed (q, mg/g) was calculated using Eq. (2):

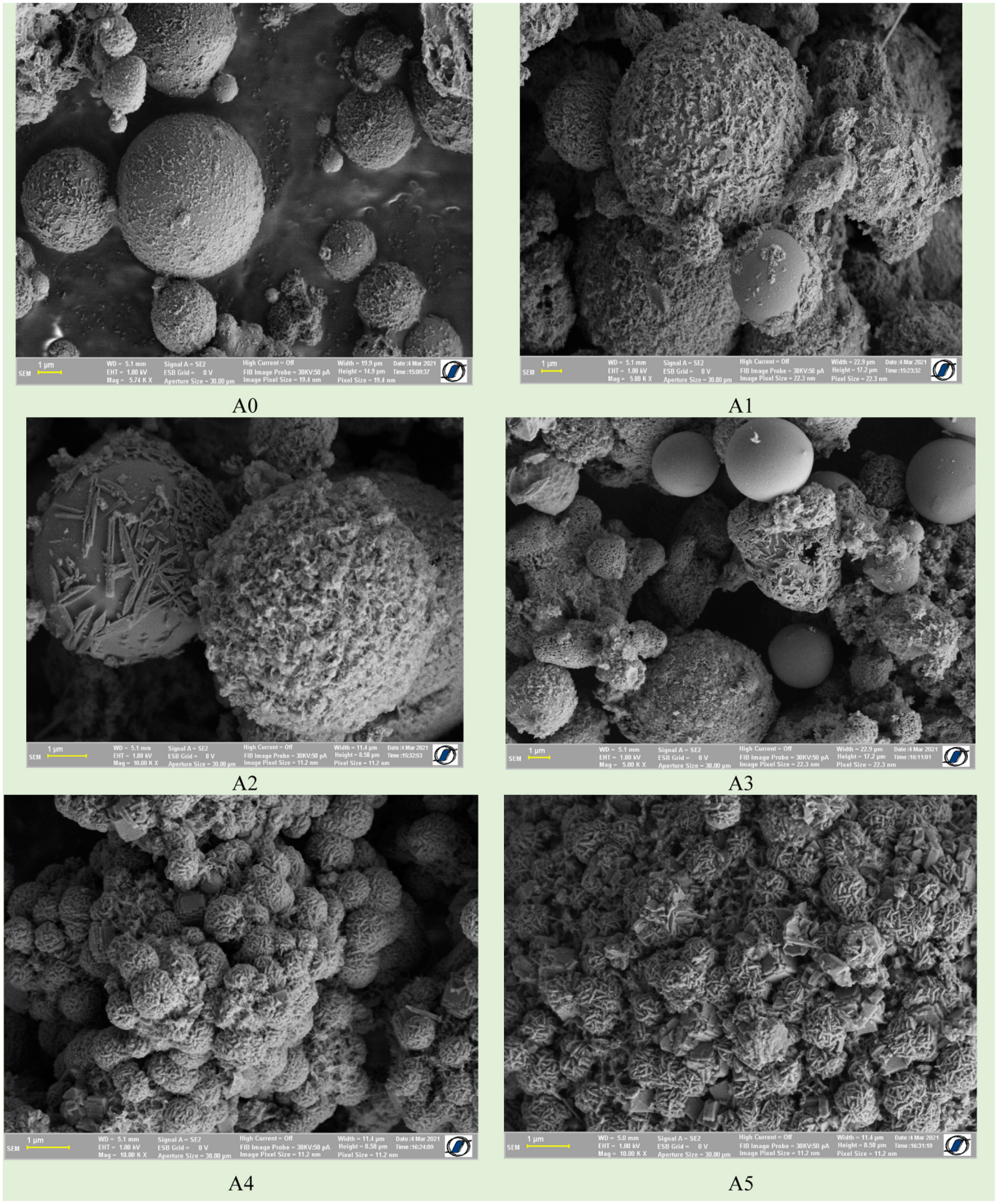

Fig. 1. SEM images for A0 vs. A1–A5.

Table 1
Method and conditions of adsorbent synthesis.

Adsorbents	Synthesis method	FA: NaOH ratio	Temperature, °C	NaOH, M	Contact time, h
A1	Direct activation	1:3	20	2	168
A2	Ultrasound	1:5	70	5	1
A3	Ultrasound	1:5	70	5	2
A4	Direct activation	1:5	90	5	4
A5	Direct activation	1:3	90	5	15

$$q, mg/g = \frac{(C_i - C_e)V}{m} \quad (2)$$

where C_i and C_e (mg/L) are the initial concentration and the concentration at equilibrium respectively, V (L) is the volume of the Cd (II) solution and m (g) is the mass of the adsorbents used.

The concentrations were measured in triplicate; the errors were up to 5%.

The Cd(II) loaded A0-A5 adsorbents was subjected to desorption study by using the toxicity characteristic leaching procedure (TCLP) at pH of 4.93 ± 0.05 (5.7 mL glacial CH_3CH_2OOH and 64.3 mL1 N NaOH diluted in 1 L distilled water - TCLP extract 1) and pH of 2.88 ± 0.05 (5.7 mL glacial CH_3CH_2OOH diluted in 1 L distilled water - TCLP extract 2). The pH values of the two solutions were adjusted with 1 mol/L HNO_3 and 1 mol/L NaOH. An aliquot of 1 g of each adsorbent and 20 mL extraction reagent were transferred into 50 mL beaker. The samples were stirred with a speed of 30 ± 2 RPM for 18 h at 25 °C. After 18 h of contact time, the supernatant was filtered and the Cd(II) concentration was determined in the TCLP extract [43].

3. Results and discussion

3.1. Characterization of adsorbents

If a material is intended for use as an adsorbent, it is important to establish certain characteristics. A fundamental analysis is the BET surface area. A larger surface area can increase the adsorption capacity. The functional groups also provide important information about the material. In this research, a SEM analysis was performed in order to obtain information about the impact of the activation and ultrasound methods on the morphology of fly ash. Thus, SEM, FTIR and BET surface area analyses were performed in order to establish the morphology, the functional groups and the specific surface values of the adsorbents studied.

Table 2
Elemental analysis of FA and synthesized materials (atomic, %).

	O	Na	Mg	Al	Si	K	Ca	Ti	Fe
A0	69.92	0.61	0.65	9.19	17.29	0.50	0.65	0.24	0.94
A1	66.99	3.20	0.66	9.32	16.23	0.77	0.82	0.34	1.67
A2	70.87	0.48	0.63	10.58	12.73	0.31	3.33	0.23	0.84
A3	69.05	0.91	0.83	11.06	14.44	0.46	1.33	0.38	1.53
A4	65.31	6.69	1.15	12.79	11.61	0.12	0.60	0.31	1.43
A5	67.78	5.67	0.47	12.14	11.09	0.12	1.10	0.66	0.96

3.1.1. SEM analysis

The SEM images of the A0–A5 adsorbents (at 1 μm) are presented in Fig. 1. (See Table 1.)

As shown in Fig. 1 the morphology of the new materials (A1–A5) differed from that of A0.

The raw FA is composed of spherical microparticles by different diameters. The FA was characterized by a mixed crystalline-amorphous structure. The synthesized materials have various morphologies, in function of synthesis conditions. The modification of A2 and A3 was less extreme. The activation of fly ash by the ultrasound method leds to the destruction of the particles. SEM images reveal nanocrystalline texture for A4 and A5, while for the samples A2 and A3 the crystallites increased on the FA surface. In the case of A4 and A5 different shapes were found: cubic crystals corresponded to Linde type zeolites, hexaoctahedral typical for Faujasite, and spherical crystals which are most likely Sodalite, in accordance with [44]. A4 and A5 presented nano- crystals in the form of elongated rods (Fig. 2).

The results of EDAX analysis are presented in Table 2.

The fly ash contains the following compounds: Si, O, Al, Fe, Ca, Mg and small quantities of Ti, K and Na. More details are presented in a

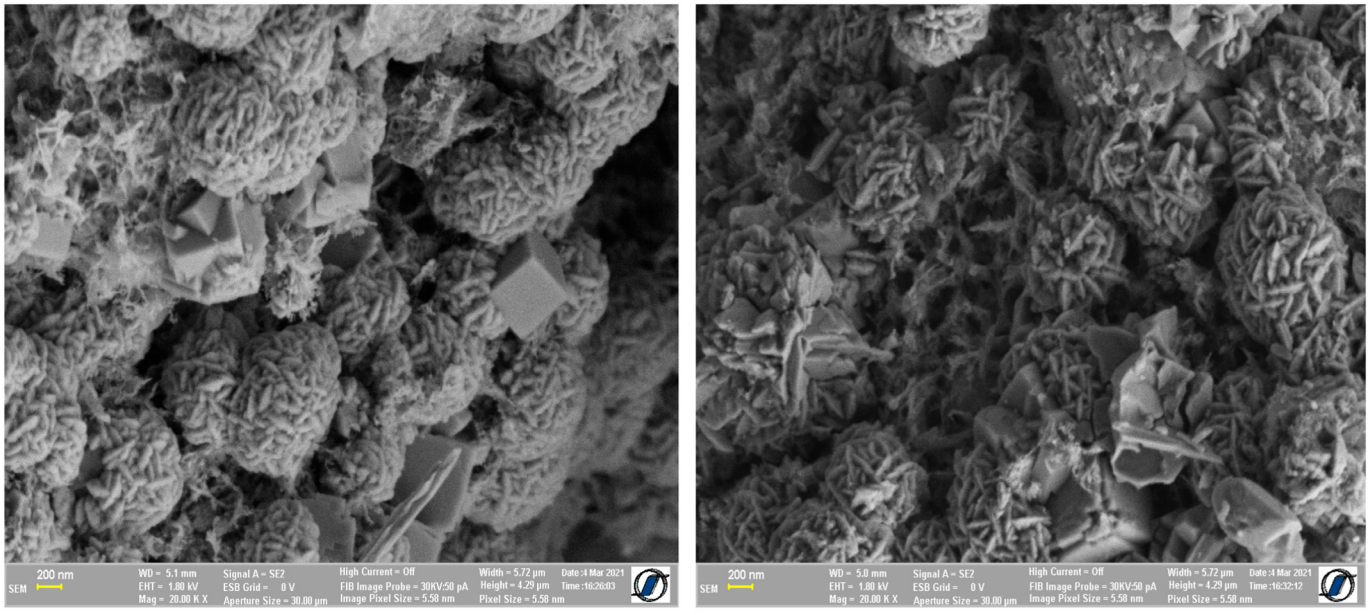

A4 A5

Fig. 2. SEM images for A4 and A5, at the 200 nm.

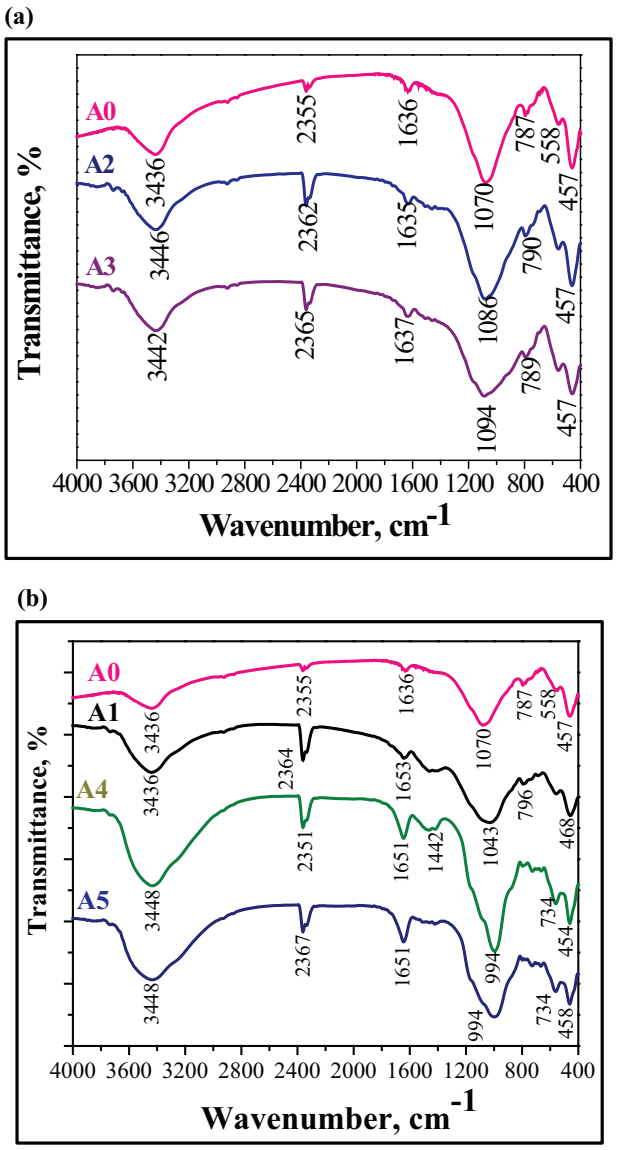

Fig. 3. a. FTIR spectra for A0 vs. A2 vs. A3. b. FTIR spectra for A0 vs. A1 vs. A4 vs. A5.

previous paper [45]. The chemical composition of the fly ash regarding the trace elements (NAA) analysis was: As = 5.11×10^1 ppm, V = 2.53×10^2 ppm, Cr = 1.27×10^2 ppm, Mn = 4.1×10^2 ppm, V = 253 ppm, and Cr < 5 ppm.

The synthesized materials have the same components as the fly ash, but from Table 2 it can be seen that the chemical composition was modified by alkaline attack, especially with refer to Na content. A long period of attack (168 h) determines chemical reactions with the increase of Na content at 3.20%. A higher quantity of Na content was obtained for FA: NaOH ratio of 1:3 and 90 °C (A5), the close content was obtained for material synthesized at reduced ratio, but with increase of attack time from 4 h to 15 h.

Table 3
BET values.

Adsorbent	A0	A1	A2	A3	A4	A5
S_{BET}, m^2/g	7.23	9.35	20.52	14.75	40.18	87.42
V_{pores} 10^{-3}, cm^3/g	24.3	42.5	90.9	68.5	124.5	136

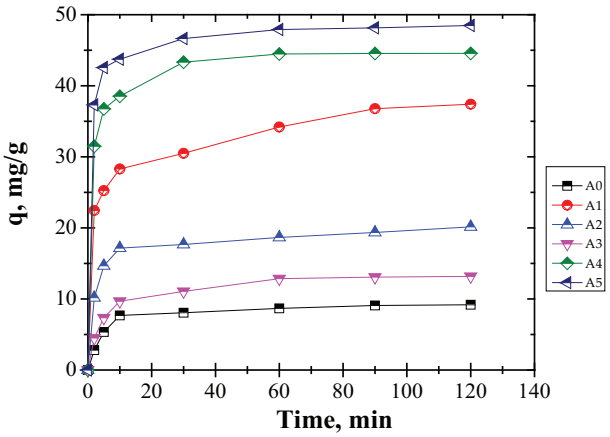

Fig. 4. Influence of contact time and type of adsorbent on Cd (II) adsorption.

3.1.2. FTIR analysis

FTIR spectra for the adsorbents studied are presented in Fig. 3(a,b), and confirmed the presence of similar peaks for all adsorbents. For example, the peaks detected at wavelengths of 454–468 cm^{-1} were O – Si – O or Si – O – Si bonds; Al – O – Al and Si – O – Si bonds were found at 558 cm^{-1}; the Si – O bond was detected between 787 and 796 cm^{-1}; the symmetric Si – O – Si group was found at 734–796 cm^{-1}; the peaks observed between 994 and 1094 cm^{-1} were attributed to Si – Al – O bonds; on the other hand, asymmetric Si – O – Si and asymmetric T – O – Si bonds(where T = Si, Al) were found at 1074–1086 cm^{-1}. The peaks at 1635–1656 cm^{-1} and 3436–3448 cm^{-1} suggest –OH and H–O–H bonds respectively.

Fig. 3a shows that in the case of materials synthesized by the ultrasound method (A2 and A3) the FTIR analysis gave similar results to that of A0, which indicates that 1 and 2 h of modification does not influence the structure of the ash. The only considerable difference between ash and the materials synthesized by the ultrasound method was the movement of the peak from 1070 cm^{-1} to 1086 cm^{-1} (in the case of A2) and 1094 cm^{-1} (in the case of A3). The FTIR analysis of A4 (Fig. 3b) demonstrated a peak at 1442 cm^{-1}, corresponding to the Na—Y zeolite.

A4 showed a peak corresponding to 2351 cm^{-1} that was more pronounced than that of A0. Fig. 2b also shows the movement of the peak from 1070 cm^{-1} to 994 cm^{-1}.

The only difference between A4 and A5 is the lack of a peak at 1442 cm^{-1}.

The FTIR analysis (Fig. 2b) showed almost identical peaks for A1 and A0, the only difference being the displacement of the peak from 1070 cm^{-1} to 1043 cm^{-1}.

3.1.3. BET surface area

The results regarding the BET analysis are shown in Table 3.

According to Table 3, A1–A5 have higher BET surface values than A0, which could explain their higher adsorption capacity, consistent with previous reports [46,47].

3.2. Adsorption experiments

To investigate the influence of contact time, the samples were collected at different pre-set time intervals ranging from 2 to 120 min. In addition, the influence of the type of adsorbent on the adsorption capacity was investigated using fly ash and six new adsorbents based on fly ash.

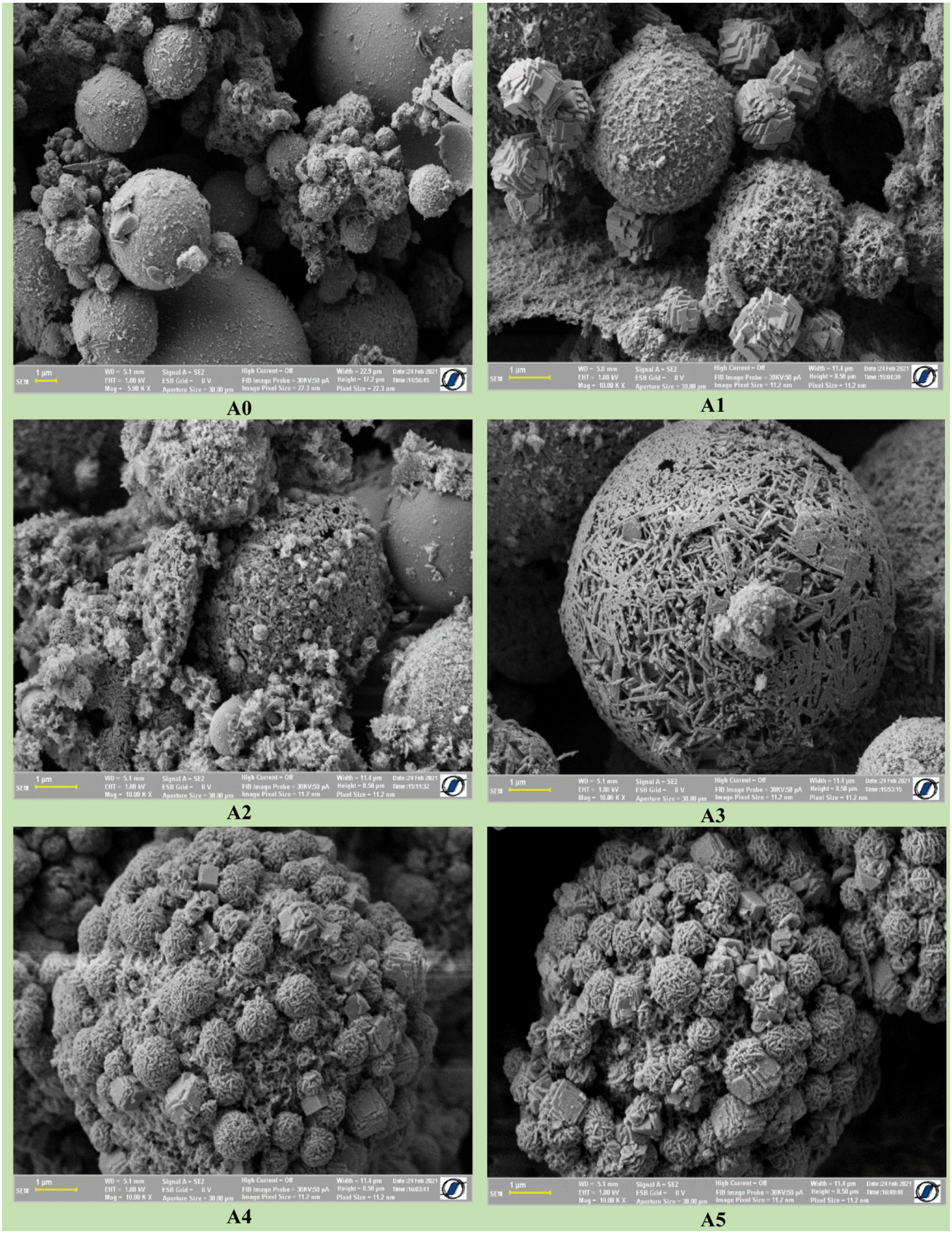

Fig. 5. a. SEM images of A0-A5 after Cd(II) adsorption process. b. SEM/EDS analysis after Cd(II) adsorption process.

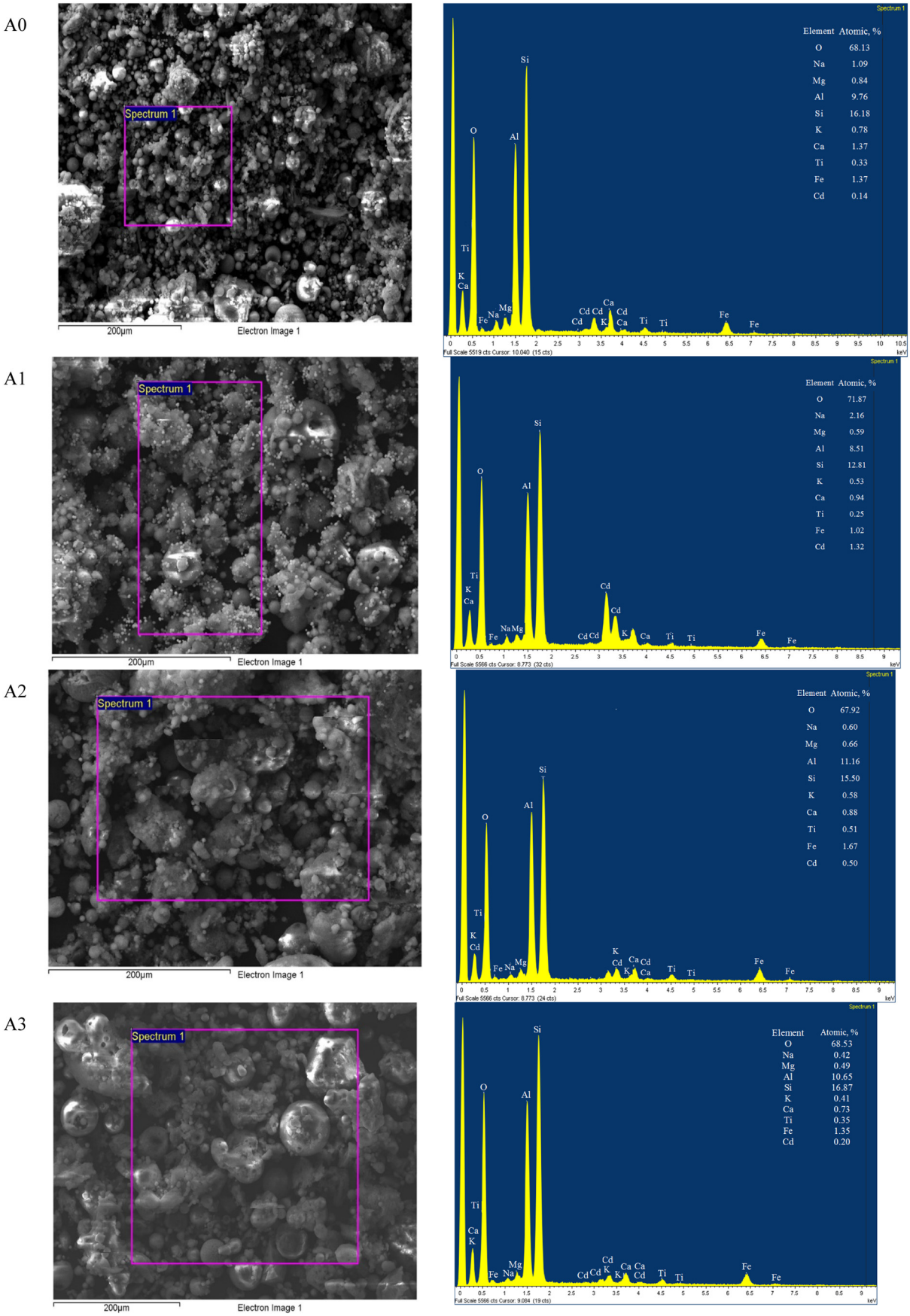

Fig. 5 (*continued*).

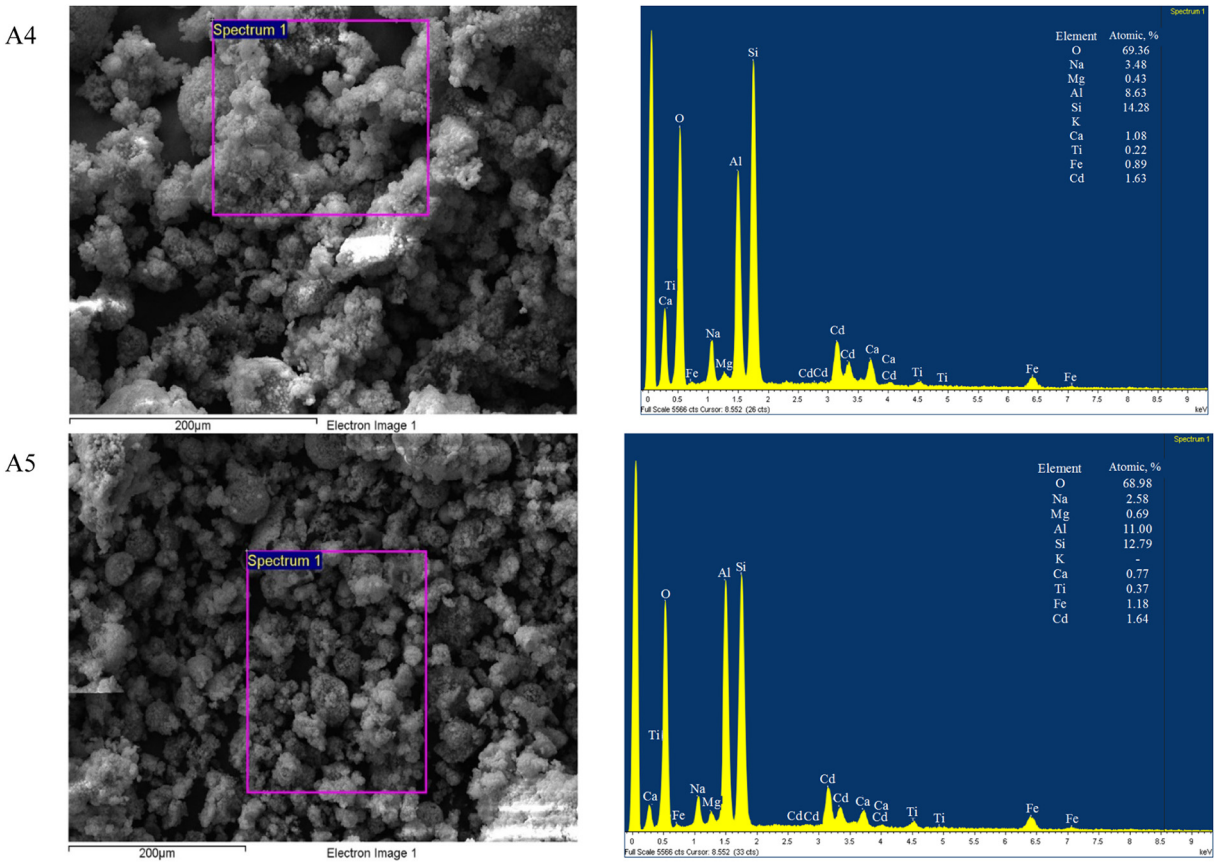

Fig. 5 (*continued*).

3.2.1. Influence of contact time

The influence of contact time is illustrated in Fig. 4. The results show that with increasing contact time, the quantity of Cd (II) ions adsorbed per unit mass of A0–A5 adsorbent increased. The adsorption process was fastest in the initial stage, with more than 60% of the total amount of Cd (II) in the aqueous solution being adsorbed in the first 30 min. A contact time of 120 min can be considered as sufficient to reach equilibrium. Given that equilibrium was reached in less than 2 h, the use of the adsorbents to eliminate Cd (II) ions from aqueous solutions appears promising. The type of adsorbent plays an important role in the adsorption process. The purpose of this study was to compare the impact of five types of adsorbents based on fly ash on Cd (II) adsorption capacity. The effect of the type of adsorbent was evaluated by comparing the materials obtained using the direct activation method (A4 and A5), the ultrasound method (A2 and A3), and the activation method without stirring at a low temperature (A1).

We found that the adsorption capacity was greatly influenced by the type of adsorbent. A0 exhibited the lowest adsorption capacity for Cd (II) ions, while A1–A5 all exhibited a higher adsorption capacity. Using the ultrasound method at the same NaOH concentration (5 M), temperature (70 °C) and 1:3 ratio of fly ash:NaOH, but with a contact time of 1 or 2 h resulted in different adsorption capacities. Analysis of the data presented in Fig. 3a,b showed that the synthesis of fly ash by the ultrasound method with 1 h of contact time led to an increase in the adsorption capacity 2.2 times higher than that of A0. A3 showed a low adsorption capacity. The destruction of the surface of the material by the ultrasound method (A3) impedes the adsorption of Cd (II) ions onto the surface of the material.

Fig. 4 highlights the high adsorption capacities of A4 and A5. The experimental results indicated the positive effect of a higher NaOH concentration (5 M), as well as a longer contact time (4 h and 15 h). Therefore, there is potential for significantly improving adsorption capacity. Also, it is important to point out that A1 shows great promise as an adsorbent for Cd (II) adsorption. The material was synthesized using an easy and low-cost experimental technique. Although the synthesis took place over a period of 7 days, a good adsorption capacity was obtained, i.e., 37.4 mg/g.

The experimental data illustrated that the adsorption of Cd (II) ions is greatly influenced by the type of adsorbent. The results obtained for the effect of the type of adsorbent showed significant differences in adsorption capacities. A4 and A5 had the highest adsorption capacity, and A0, A2 and A3 had the lowest adsorption capacity: A0 < A3 < A2 < A1 < A4 < A5.

The SEM/EDS and FTIR analysis were also carried out in order to examine the samples after Cd(II) adsorption. The Fig. 5a depicts the morphology of fly ash and synthesized materials after Cd(II) adsorption process. From Fig. 5a it can be seen that after adsorption the materials have the same morphology as the initial materials, but new phase, in the shape of sheet appear especially in the case of A1, A4 and A5 samples. These phases are hydrates compounds and the new phases reached in cadmium.

From the SEM images it can be stated that after adsorption new phases were formed at the surface of adsorbents [48]. The chemical composition of the Cd(II) loaded adsorbents, given by EDS analysis, demonstrate that Cd(II) ions were attached to the adsorbent surface.

The EDS analysis demonstrated the presence of Cd(II) on the analyzed surfaces of the adsorbents after Cd(II) adsorption process, Fig. 5b.

FTIR analysis of Cd(II) loaded adsorbents was performed in order to establish the functional groups involved in the interactions between the Cd(II) and A0-A5 adsorbents surface, Fig. 6.

From the Fig. 6 it can be seen some new significant peaks in comparison with the FTIR spectra of the adsorbents before the Cd(II) adsorption process (Fig. 3a, b). The significant peaks are presented in Table 4.

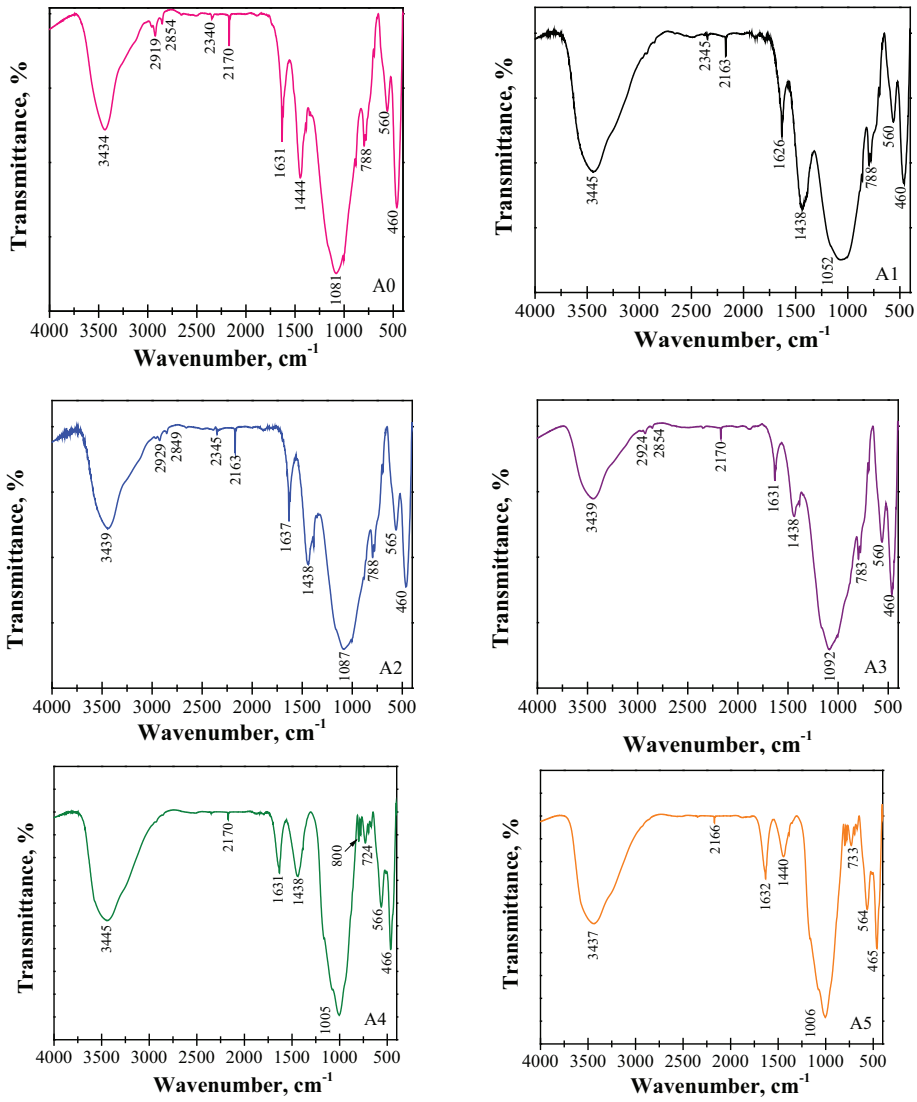

Fig. 6. FTIR analysis after Cd(II) adsorption process.

The results presented in Table 4 show that synthesized materials are modified after Cd(II) adsorption by exchanging their monovalent cations with Cd^{2+} cations. This affirmation is validated by EDS analysis. For example, in the case of A4 the Na^{+} content decreases from 6.69% at 3.46%, and in the case of A5 from 5.67% at 2.58%, these samples having higher adsorption capacities. The FTIR spectra after adsorption, presented the characteristic bands of initial materials, but also new peaks. The explanation could be that Cd(II) ions were bound during the adsorption onto the material's surface, and the presence of new phases corresponding to calcium silicate hydrates.

The adsorption capacities obtained during this study were compared with the maximum adsorption capacities of different adsorbents available in the literature, as presented in Table 5.

3.2.2. Adsorption kinetic study

In order to obtain information regarding the kinetics of the adsorption process, the experimental data obtained were modeled using three kinetic models: pseudo first-order, pseudo second-order model, and the intraparticle diffusion model. The equations of the three kinetics models in the linear form can be written as follows [59,60]:

Table 4
Peaks of A0-A5 before and after Cd(II) adsorption, cm^{-1}.

Before adsorption	Functional groups	After adsorption	Functional groups
454–468	O – Si – O or Si – O – Si bonds	460–466	O – Si – O or Si – O – Si bonds
558	Al – O – Al and Si – O – Si bonds	560–566	Al – O – Al and Si – O – Si bonds
787–796	Si – O bond	783–788	Si – O bond
734	the symmetric Si – O – Si group	724–733	the symmetric Si – O – Si group
994–1094	Si – Al – O bonds	1005, 1006	Si – Al – O bonds
1074–1094	asymmetric Si – O – Si and asymmetric Al – O – Si bonds	1052–1092	asymmetric Si – O – Si and asymmetric Al – O – Si bonds
1635–1653	O–H	1626–1637	O–H
3436–3448	H–O–H	1438–1444	the bands can be assigned to
		2163–2170	various vibrations of silica and
		2340–2345	alumina tetrahedral in relation
		2845–2854	with Cd(II) ions, calcium
		2919–2929	silicate hydrates
		3437–3445	H–O–H

Table 5
Comparison of adsorption capacities for different adsorbents for Cd (II) adsorption.

Adsorbent	pH	Adsorbent dose, g/L	Initial concentration, mg/L	q, mg/g	Reference
Coffee grounds	5	5	100	16.45	[49]
Fe_3O_4/SC	6.5	2	10, 30, 50	3.76–12.18	[50]
Mg-Fe Layered Double Hydroxide (LDH)	6.5	0.8	50	25.6	[51]
Alkali activated fly ash	6	2	100	46.64	[52]
FA/H_2SO_4	5	8	70	5.2	[8]
FA zeolites	5	0.08	50	16.58	[53]
Natural zeolite	6	20	7	80	[54]
$CoFe_2O_4$/carboxymethyl cellulose	5	8	70	35	[55]
Polyelectrolyte-Coated Industrial Waste Fly Ash	9	4	2	0.6052	[56]
Zeolite	5	1	100	47.5	[57]
Ash/GO/Fe_3O_4 nanocomposite	6	1	10	11.185	[58]
A0	5	3	250	9.18	This study
A1	5	3	250	37.4	This study
A2	5	3	250	20.15	This study
A3	5	3	250	13.18	This study
A4	5	3	250	46.56	This study
A5	5	3	250	48.48	This study

$$\log(q_e - q_t) = \log q_e - \frac{(k_1 t)}{2.303}, \quad (3)$$

$$\frac{t}{q_t} = \frac{1}{k_2 {q_e}^2} + \frac{t}{q_e}, \quad (4)$$

$$q_t = k_i t^{0.5} + c, \quad (5)$$

where q_t (mg/g) is the amount of Cd (II) ions adsorbed at time t, q_e (mg/g) is the amount of Cd (II) ions adsorbed at equilibrium, k_1 is the pseudo first-order rate constant (1/min), k_2 is the pseudo second-order rate constant (g/mg·min); and k_i is the intraparticle diffusion rate constant.

The pseudo first-order model given by eq. (3) hypothesizes that the speed of the adsorption process is directly proportional to the difference between the initial concentration and the concentration of the adsorbate at different time "t". The pseudo second-order model expressed by Eq. (4) supposes that chemisorption is the rate controlling step and the adsorption is due to physicochemical interactions between the adsorbate/adsorbent phases. The intraparticle diffusion model, Eq. (5), assumes the rate of adsorption is dependent on the speed at which the metal diffuses onto the adsorbent surface.

The kinetic fitting for the adsorption of Cd (II) by A0–A5 is presented in Figs. 7–9.

The parameters obtained by the fitting of the experimental data are presented in Table 6. As shown, the adsorption of Cd (II) onto the adsorbents studied followed the typical pseudo second-order model.

The correlation coefficient, R^2, exceeded 0.99, and was higher than the values of the other two models studied. On the other hand, the fitting of the pseudo second-order model indicated that chemisorption is responsible for the adsorption of Cd (II) ions onto the A0–A5 materials.

Taking into consideration that the pseudo second-order model showed the best fit to the results, the model was linearized into four different types, and the values obtained are presented in Table 7.

3.2.3. Adsorption isotherm study

A5 was selected to study the Cd (II) adsorption equilibrium. The influence of an initial concentration of Cd (II) solution of up to 8 g/L at pH 5 on the adsorption of Cd (II) ions onto A5 is shown in Fig. 10. The adsorption of Cd (II) was dependent on the initial concentration of the solution. The adsorption capacity increased from 12.44 mg Cd/g to 42.5 mg Cd/g when the initial concentration increased from 100 to 350 mg/L.

By studying the adsorption equilibrium, essential physico-chemical data can be obtained for evaluating the applicability of an adsorption process and its design.

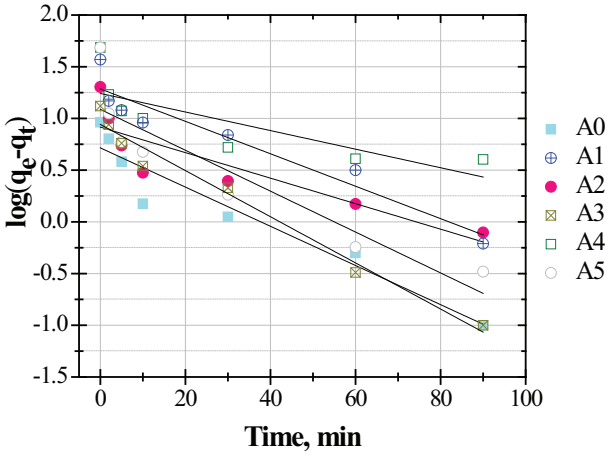

Fig. 7. The fitting of the pseudo first-order model.

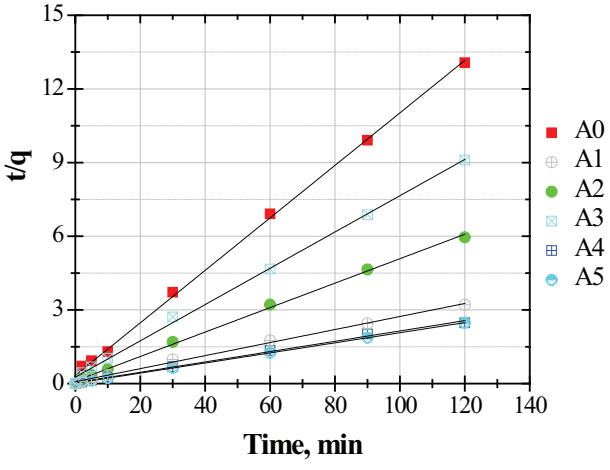

Fig. 8. The fitting of the pseudo second-order model.

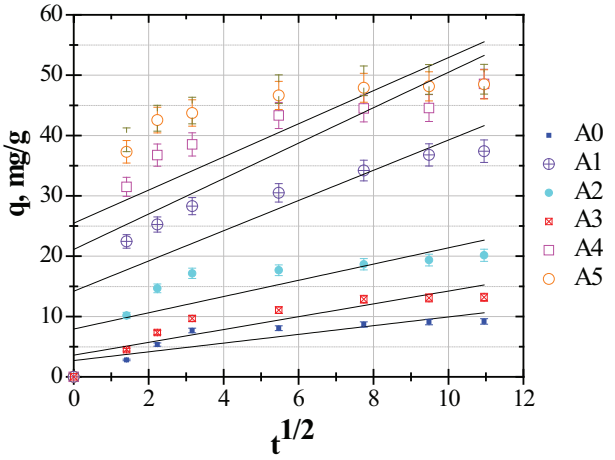

Fig. 9. The fitting of the intraparticle diffusion model.

The relationship between the amount adsorbed and that remaining in the equilibrium solution at a given temperature is the adsorption isotherm, the parameters of which express the surface properties and affinity of the adsorbent [61].

The equilibrium data were analyzed in terms of the Langmuir (four types of linearization), Freundlich, Temkin, Harkin-Jura, and Halsey isotherms, according to Eqs. 6–10 [62–65]. The adsorption isotherms for the adsorption of Cd (II) ions from solution onto the A5 material were obtained graphically, representing C_e/q_e vs. C_e (Langmuir isotherm Type 1), $1/q_e$ vs. $1/C_e$ (Langmuir isotherm Type 2), q_e vs. q_e/C_e (Langmuir isotherm Type 3), q_e/C_e vs. q_e (Langmuir isotherm Type 4), ln q_e vs. C_e (Freundlich isotherm), ln q_e vs. ln C_e (Temkin isotherm), log C_e vs. $1/q_e^2$ (Harkin-Jura isotherm), and ln C_e vs. ln q_e (Halsey isotherm).

Langmuir Type 1

$$\frac{C_e}{q_e} = \frac{1}{K_L q_{max}} + \frac{C_e}{q_{max}} \tag{6a}$$

Langmuir Type 2

$$\frac{1}{q_e} = \left(\frac{1}{q_{max} K_L}\right)\frac{1}{C_e} + \frac{1}{q_{max}} \tag{6b}$$

Table 7
Pseudo second-order kinetic model linear forms.

Kinetic model	Parameters	Values					
		A0	A1	A2	A3	A4	A5
Type I	*qe* (mg/g)	9.18	37.4	20.15	13.18	46.56	48.5
	k (g/mg min)	0.035	0.009	0.023	0.021	0.019	0.028
	R^2	**0.995**	**0.991**	**0.998**	**0.998**	**0.999**	**0.999**
Type II	*qe* (mg/g)	10.01	34.01	19.76	13.33	44.05	47.85
	k (g/mg min)	0.02	0.0254	0.0272	0.019	0.0268	0.0358
	R^2	0.9845	0.8408	0.9894	0.9972	0.9562	0.9699
Type III	*qe* (mg/g)	9.57	34.55	19.703	13.42	44.735	47.937
	k (g/mg min)	0.0247	0.023	0.0278	0.0185	0.0244	0.035
	R^2	0.9136	0.768	0.9684	0.9844	0.9141	0.9589
Type IV	*qe* (mg/g)	9.79	35.71	19.79	13.46	45.01	48.06
	k (g/mg min)	0.022	0.017	0.0268	0.0181	0.0221	0.0334
	R^2	0.9136	0.768	0.9684	0.9844	0.9141	0.9589

Langmuir Type 3

$$q_e = q_{max} - \left(\frac{1}{K_L}\right)\frac{q_e}{C_e} \tag{6c}$$

Langmuir Type 4

$$\frac{q_e}{C_e} = K_L q_{max} - K_L q_e \tag{6d}$$

Freundlich

$$\log q_e = \left(\frac{1}{n}\right)\log C_e + \log K_F \tag{7}$$

Temkin

$$q_e = \left(\frac{RT}{b}\right)\ln K_T + \left(\frac{RT}{b}\right)\ln C_e \tag{8}$$

Harkin-Jura

$$\frac{1}{q_e^2} = \frac{B_{HJ}}{A_{HJ}} - \left(\frac{1}{A_{HJ}}\right) log\, C_e \tag{9}$$

Table 6
Parameters of the kinetic models.

Adsorbent	Kinetic model		
	Pseudo first-order	Pseudo second-order	Intraparticle diffusion model
A0	$R^2 = 0.919$	**$R^2 = 0.995$** $q_e = 9.18$ $k_2 = 0.035$	$R^2 = 0.737$
A1	$R^2 = 0.914$	**$R^2 = 0.991$** $q_e = 37.4$ $k_2 = 0.009$	$R^2 = 0.688$
A2	$R^2 = 0.780$	**$R^2 = 0.998$** $q_e = 20.15$ $k_2 = 0.023$	$R^2 = 0.637$
A3	$R^2 = 0.976$	**$R^2 = 0.998$** qe = 13.18 $k^2 = 0.021$	$R^2 = 0.803$
A4	$R^2 = 0.632$	**$R^2 = 0.996$** $q_e = 46.56$ $k_2 = 0.019$	$R^2 = 0.575$
A5	$R^2 = 0.831$	**$R^2 = 0.999$** $q_e = 48.5$ $k_2 = 0.028$	$R^2 = 0.452$

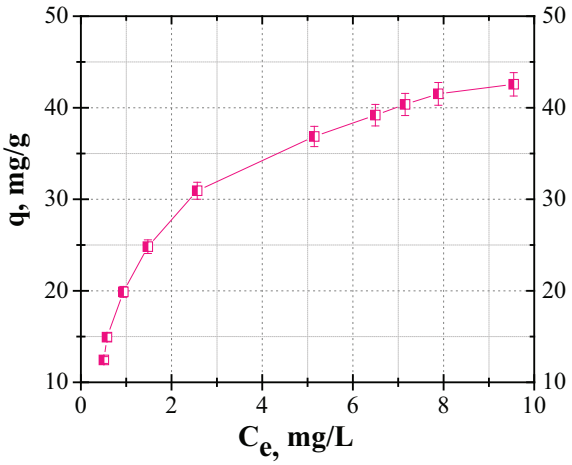

Fig. 10. Influence of initial concentration.

Halsey

$$\ln q_e = \left(\frac{1}{n_H}\right) \ln K_H - \left(\frac{1}{n_H}\right) \ln lnC_e \quad (10)$$

The correlations between the experimental results obtained for Cd (II) adsorption on the studied material and the isotherms are presented in Figs. 11–15. The values of the adsorption isotherm constants calculated from the intercept and slope are given in Table 8. The equilibrium model that best describes Cd (II) adsorption on A5 was based on the linear regression coefficients, R^2.

Where: q_{max} is the maximum adsorption capacity (mg/g); K_L is the Langmuir constant (L/g); K_F is the Freundlich constant; 1/n is the heterogeneity factor; A_T is the Temkin isotherm equilibrium binding constant (L/g); b_T is the Temkin isotherm constant; B is the constant related to heat of adsorption (J/mol); A_{HJ} and B_{HJ} are Harkin-Jura constants, and n_H and k_H are Halsey isotherm constants.

After comparing the values of the regression coefficients (R^2) it can be concluded that the Langmuir Type 1 model most successfully described the experimental data.

The adsorption of Cd (II) did not fit the Harkin-Jura model, which had a low R^2 of 0.7872.

On the other hand, the value of 2.58 for n calculated from the Freundlich isotherm indicated the good efficiency of A5 for cadmium adsorption [66].

3.2.4. Desorption study

The desorption experiments of the Cd(II) loaded A0-A5 adsorbents were performed in order to investigate the reusability and the environmental compatibility during their disposal. In this reason, consecutive adsorption and desorption cycles were performed for 4 times, the adsorption efficiency decreasing from 92% at 60%. On the other hand the obtained results of the TCLP method, using extract 1 and extract 2 are shown in the Fig. 15.

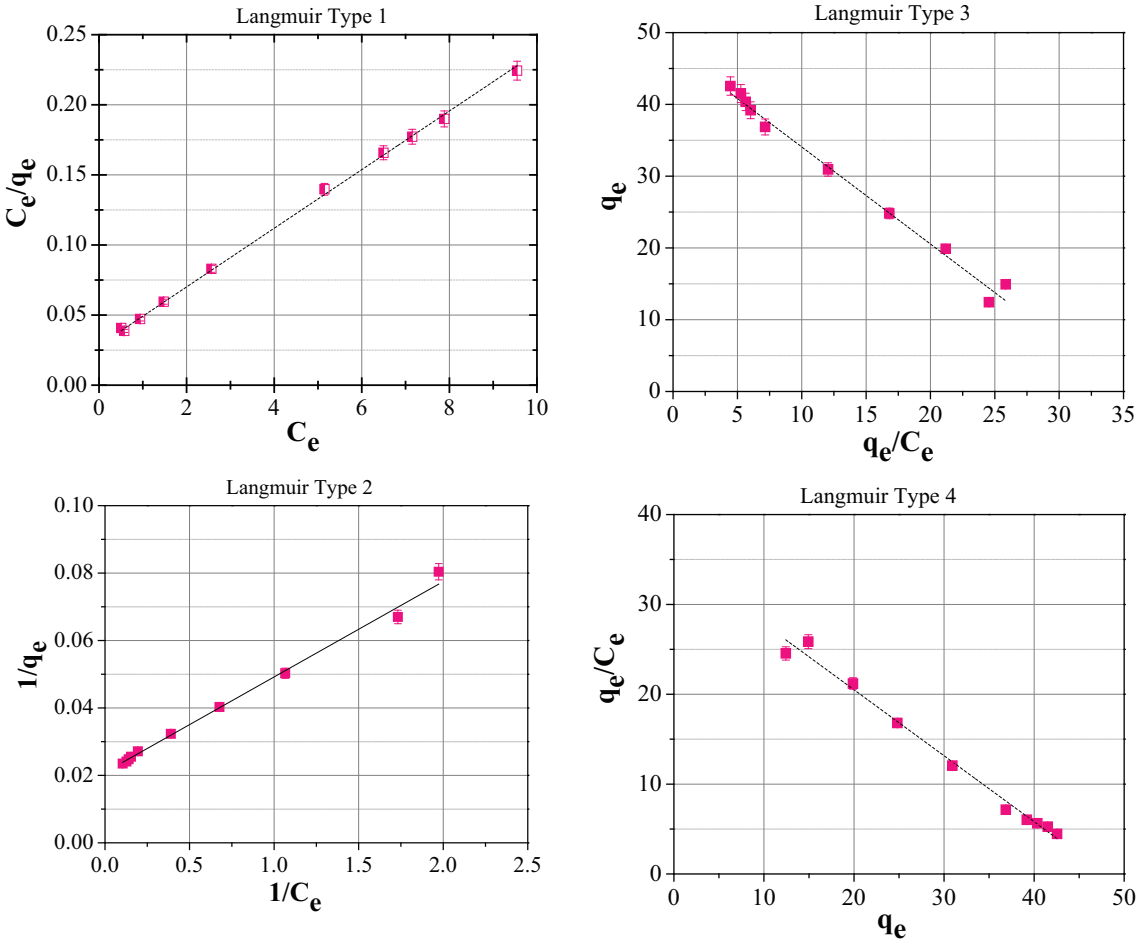

Fig. 11. Langmuir isotherm.

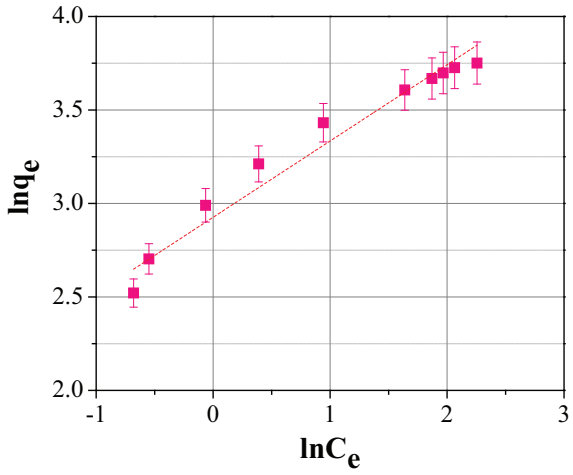

Fig. 12. Freundlich isotherm.

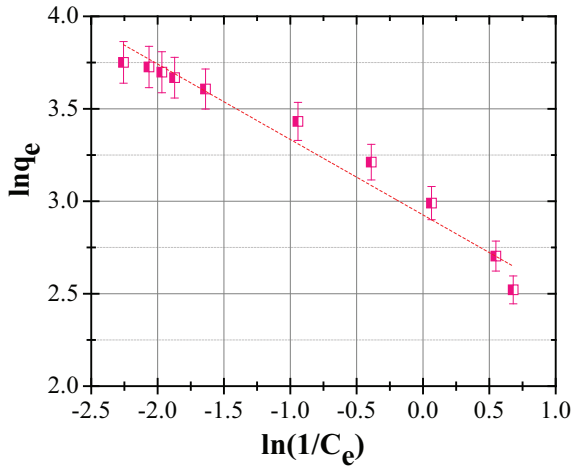

Fig. 15. Halsey isotherm.

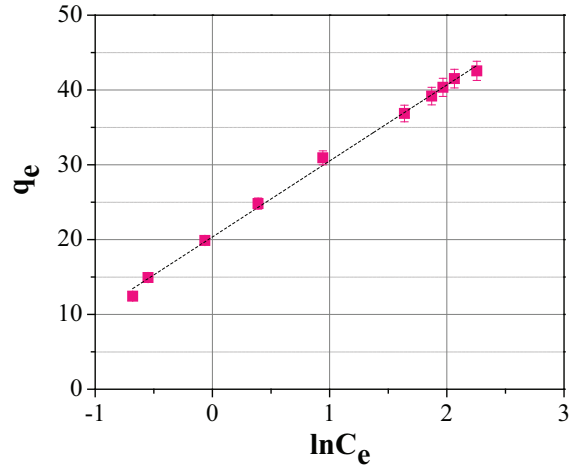

Fig. 13. Temkin isotherm.

Table 8
Adsorption isotherm constants.

Langmuir Type 1	q_{max}, mg/g	48.31
	K_L (L/mg)	0.7089
	R^2	0.991
Langmuir Type 2	q_{max}, mg/g	48.08
	K_L (L/mg)	0.7272
	R^2	0.9936
Langmuir Type 3	q_{max}, mg/g	47.72
	K_L (L/mg)	0.7423
	R^2	0.989
Langmuir Type 4	q_{max}, mg/g	47.91
	K_L (L/mg)	0.7342
	R^2	0.989
Freundlich	K_F	18.99
	1/n	0.3931
	R^2	0.9649
Temkin	B	10.156
	b	243.95
	A_T	1.63
	R^2	0.9975
Harkin-Jura	A_{HJ}	270.27
	B_{HJ}	0.95
	R^2	0.7872
Halsey	n_H	2.54
	k_H	1636
	R^2	0.9649

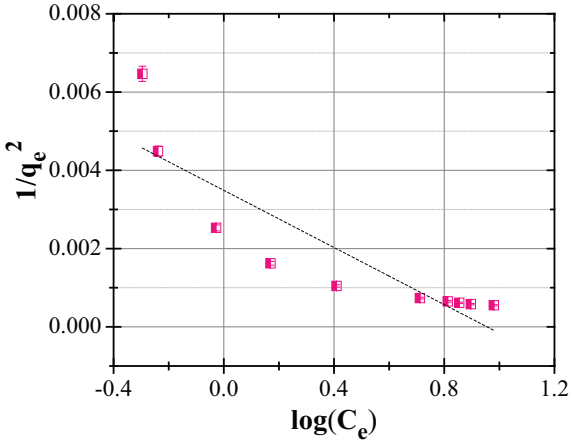

Fig. 14. Harkin-Jura isotherm.

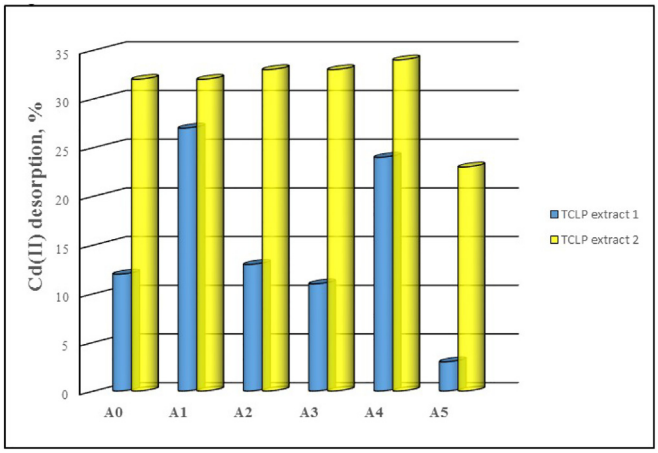

Fig. 16. Desorption of Cd(II) from A0-A5 adsorbents.

From Fig. 16 it can be seen that the percentage concentration of the Cd(II) cations in the leachate of A0 varied from approximately 12 to 32%, respectively. The A5 adsorbent had the desorption percentage from 4% to 22%, it means that Cd(II) was bonded into adsorbent bulk. The published data with reference to desorption studies are reduced, but our results are in good agreement with those of other researchers [67,68].

4. Conclusions

The use of five adsorbents based on fly ash treated with NaOH by direct activation and ultrasound methods for the adsorption of cadmium ions from aqueous solutions was investigated. The materials were characterized using SEM, FTIR and BET methods. Also, SEM/EDS and FTIR analysis after Cd(II) adsorption were investigated.

The effect of contact time and type of adsorbent was investigated first. The results showed that Cd (II) adsorption is dependent on contact time and type of adsorbent. The adsorbents prepared demonstrated good capacity for adsorption of Cd (II) from aqueous solutions under experimental conditions. The maximum adsorption capacities obtained were in the range of 9.18–48.5 mg/g.

The results of the kinetic study showed that the adsorption of Cd (II) ions proceeds rapidly in the first 10 min, and that equilibrium is reached in less than 2 h.

The experimental data were used for kinetics determination using three model equations: pseudo first-order model, pseudo second-order model, and the intraparticle diffusion model. We found that the adsorption of Cd (II) onto the adsorbents studied follows the pseudo second-order model.

The experimental data were also processed using the Langmuir (four types of linearization), Freundlich, Temkin, Harkin-Jura, and Halsey adsorption isotherms. The data for A5 fitted the Langmuir model, Type 1.

Overall, the results highlight that all materials investigated have the potential to adsorb Cd (II) ions, with an efficiency ranked as follows: A0 < A3 < A2 < A1 < A4 < A5.

The synthesized materials can be used for the 4 adsorption-desorption cycles, with the proper efficiency. The A5 adsorbent had a desorption percentage of Cd(II) at pH of 4.93 ± 0.05, confirmed by TCLP test.

The chemical technologies for treating contaminated waters need to be feasible. Fly ash conversion is recommended both to solve the problems associated with its storage and to clean wastewaters containing cadmium.

Funding

This research was funded by the UEFISCDI Agency trough Project PN-III-P1–1.2-PCCDI-2017-0152 (Contract No. 75PCCDI/2018).

Author statement

Gabriela Buema: Methodology, Software, Investigation. **Nicoleta Lupu:** Data curation, Formal analysis, Investigation. **Horia Chiriac:** Conceptualization, Visualization, Supervision. **Gabriela Ciobanu:** Writing - original draft, Investigation. **Roxana-Dana Bucur:** Software, Validation, Investigation. **Daniel Bucur:** Methodology, Investigation, Formal analysis. **Lidia Favier:** Data curation, Investigation. **Maria Harja:** Supervision, Methodology, Writing- Original draft, Validation, Writing - review & editing.

Declaration of Competing Interest

The authors declare no conflict of interest.

References

[1] S. Jorfi, M.R. Shooshtarian, S. Pourfadakari, Decontamination of cadmium from aqueous solutions using zeolite decorated by Fe_3O_4 nanoparticles: adsorption modeling and thermodynamic studies, Int. J. Environ. Sci. Technol. 17 (1) (2020) 273–286, https://doi.org/10.1007/s13762-019-02350-2.

[2] V. Kumar, A. Sharma, R. Kumar, R. Bhardwaj, A. Kumar Thukral, J. Rodrigo-Comino, Assessment of heavy-metal pollution in three different Indian water bodies by combination of multivariate analysis and water pollution indices, Hum. Ecol. Risk. Assess. 26 (2020) 1–16, https://doi.org/10.1080/10807039.2018.1497946.

[3] J. Ulatowska, Ł. Stala, A. Nowakowska, I. Polowczyk, Use of synthetic zeolite materials from fly ash to remove copper(II) ions from aqueous solutions, Physicochem. Probl. Miner. Process. 56 (2020) 114–124, https://doi.org/10.37190/ppmp/127061.

[4] K.S. Hui, C.Y.H. Chao, S.C. Kot, Removal of mixed heavy metal ions in wastewater by zeolite 4A and residual products from recycled coal fly ash, J. Hazard. Mater. B127 (2005) 89–101, https://doi.org/10.1016/j.jhazmat.2005.06.027.

[5] K.H. Vardhan, P.S. Kumar, R.C. Panda, A review on heavy metal pollution, toxicity and remedial measures: current trends and future perspectives, J. Mol. Liq. 290 (2019) 111197, https://doi.org/10.1016/j.molliq.2019.111197.

[6] I.A. Perovskiy, N.Y. Yanicheva, V.V. Stalyugin, T.L. Panikorovskii, A.A. Golov, Sorption of multivalent cations on titanosilicate obtained from natural raw materials. The mechanism and thermodynamics of sorption, Microporous Mesoporous Mater. 311 (2020), 110716, https://doi.org/10.1016/j.micromeso.2020.110716.

[7] G. Buema, M. Harja, N. Lupu, H. Chiriac, L. Forminte, G. Ciobanu, D. Bucur, R.D. Bucur, Adsorption performance of modified Fly ash for copper ion removal from aqueous solution, Water 13 (2021) 207, https://doi.org/10.3390/w13020207.

[8] G. Buema, N. Lupu, H. Chiriac, T. Roman, M. Porcescu, G. Ciobanu, D.V. Burghila, M. Harja, Eco-friendly materials obtained by fly ash sulphuric activation for heavy metals removal, Materials 13 (16) (2020) 3584, https://doi.org/10.3390/ma13163584.

[9] F. Noli, G. Buema, P. Misaelides, M. Harja, New materials synthesized from ash under moderate conditions for removal of toxic and radioactive metals, J. Radioanal. Nucl. Chem. 303 (2015) 2303–2311, https://doi.org/10.1007/s10967-014-3762-1.

[10] G. Buema, G. Lisa, O. Kotova, G. Ciobanu, L. Ivaniciuc, L. Favier, M. Harja, Application of thermal analysis to improve the preparation conditions of zeolitic materials from flying ash, Environ. Eng. Manag. J. 20 (3) (2021) 377–388.

[11] H. Shen, Y. Wu, M. Zhou, S.T. Smith, H. Zhang, G. Yue, Identification of the initial particle size distribution for coal combustion simulations, AICHE J. 65 (8) (2019), e16610, https://doi.org/10.1002/aic.16610.

[12] S. Dash, H. Chaudhuri, R. Gupta, U.G. Nair, Adsorption study of modified coal fly ash with sulfonic acid as a potential adsorbent for the removal of toxic reactive dyes from aqueous solution: kinetics and thermodynamics, J. Env. Chem. Eng. 6 (5) (2018) 5897–5905, https://doi.org/10.1016/j.jece.2018.05.017.

[13] A. Bhatt, S. Priyadarshini, A.A. Mohanakrishnan, A. Abri, M. Sattler, S. Techapaphawit, Physical, chemical, and geotechnical properties of coal fly ash: a global review, Case Stud. Constr. Mater. 11 (2019), e00263, https://doi.org/10.1016/j.cscm.2019.e00263.

[14] Y. Luo, S. Zheng, S. Ma, C. Liu, X. Wang, Ceramic tiles derived from coal fly ash: preparation and mechanical characterization, Ceram. Int. 43 (15) (2017) 11953–11966, https://doi.org/10.1016/j.ceramint.2017.06.045.

[15] S. You, S.W. Ho, T. Li, T. Maneerung, C.H. Wang, Techno-economic analysis of geopolymer production from the coal fly ash with high iron oxide and calcium oxide contents, J. Hazard. Mater. 361 (2019) 237–244, https://doi.org/10.1016/j.jhazmat.2018.08.089.

[16] P.O. Awoyera, M.S. Kirgiz, A. Viloria, D. Ovallos-Gazabon, Estimating strength properties of geopolymer self-compacting concrete using machine learning techniques, J. Mater. Res. Technol. 9 (4) (2020) 9016–9028, https://doi.org/10.1016/j.jmrt.2020.06.008.

[17] M. Harja, S.M. Cimpeanu, M. Dirja, D. Bucur, Synthesis of zeolites from fly ash and their use as soil amendment, Zeolites - Useful Minerals, IntechOpen, London, 2016.

[18] M. Merzouki, R. Kachkoul, H. Belhassan, Y. Miyah, H. Amakdouf, R. Elmountassir, A. Lahrichi, Fixed-bed adsorption of tannery wastewater pollutants using bottom ash: an optimized process, Surf. Interfaces 22 (2021) 100868, https://doi.org/10.1016/j.surfin.2020.100868.

[19] F.A. Al-Khaldi, B. Abusharkh, M. Khaled, M.A. Atieh, M.S. Nasser, T.A. Saleh, V.K. Gupta, Adsorptive removal of cadmium (II) ions from liquid phase using acid modified carbon-based adsorbents, J. Mol. Liq. 204 (2015) 255–263, https://doi.org/10.1016/j.molliq.2015.01.033.

[20] A. Derkowski, W. Franus, E. Beran, A. Czimerova, Properties and potential applications of zeolitic materials produced from fly ash using simple method of synthesis, Powder Technol. 166 (2006) 47–54, https://doi.org/10.1016/j.powtec.2006.05.004.

[21] N. Djamel, A. Samira, Mechanism of Cu^{2+} ions uptake process by synthetic NaA zeolite from aqueous solution: characterization, kinetic, intra-crystalline diffusion and thermodynamic studies, J. Mol. Liq. 323 (2021) 114642, https://doi.org/10.1016/j.molliq.2020.114642.

[22] L. Forminte, G. Ciobanu, G. Buema, N. Lupu, H. Chiriac, C. Gomez de Castro, M. Harja, New materials synthesized by sulfuric acid attack over power plant fly ash, Rev. Chim. 71 (7) (2020) 48–58.

[23] B.K. Saikia, J.C. Hower, N. Islam, A. Sharma, P. Das, Geochemistry and petrology of coal and coal fly ash from a thermal power plant in India, Fuel 291 (2021), 120122, https://doi.org/10.1016/j.fuel.2020.120122.

[24] R.I. Birley, J.M. Jones, L.I. Darvell, A. Williams, D.J. Waldron, Y.A. Levendis, E. Rokni, A. Panahi, Fuel flexible power stations: utilisation of ash co-products as additives

for NO_x emissions control, Fuel 251 (2019) 800–807, https://doi.org/10.1016/j.fuel.2019.04.002.
[25] G. Buema, N. Lupu, H. Chiriac, G. Ciobanu, O. Kotova, M. Harja, Modeling of solid-fluid non-catalytic processes for nickel ion removal, Rev. Chim. 71 (7) (2020) 4–15.
[26] N. Czuma, I. Casanova, P. Baran, J. Szczurowski, K. Zarębska, CO_2 sorption and regeneration properties of fly ash zeolites synthesized with the use of differentiated methods, Sci. Rep. 10 (2020) 1825, https://doi.org/10.1038/s41598-020-58591-6.
[27] Z. Hussain, G. Lizhen, M. Moeen, Treatment of coal Fly ash and environmentally friendly use with rubber in cable wires as insulation material, Sustainability 12 (2020) 5218, https://doi.org/10.3390/su12125218.
[28] M. Harja, G. Buema, N. Lupu, H. Chiriac, D.D. Herea, G. Ciobanu, Fly ash coated with magnetic materials: improved adsorbent for cu (II) removal from wastewater, Materials 14 (1) (2021) 63, https://doi.org/10.3390/ma14010063.
[29] N. Ghazali, K. Muthusamy, S.W. Ahmad, Utilization of Fly ash in construction, IOP Conf. Series: Mat. Sci. Eng. 601 (2019), 012023, https://doi.org/10.1088/1757-899X/601/1/012023.
[30] M. Harja, G. Buema, L. Bulgariu, D. Bulgariu, D.M. Sutiman, G. Ciobanu, Removal of cadmium (II) from aqueous solution by adsorption onto modified algae and ash, Korean J. Chem. Eng. 32 (9) (2015) 1804–1811, https://doi.org/10.1007/s11814-015-0016-z.
[31] A. Assi, F. Bilo, A. Zanoletti, J. Ponti, A. Valsesia, R. La Spina, L.E. Depero, E. Bontempi, Review of the reuse possibilities concerning ash residues from thermal process in a medium-sized urban system in northern Italy, Sustainability 12 (2020) 4193, https://doi.org/10.3390/su12104193.
[32] H. Tang, X. Xu, B. Wang, C. Lv, D. Shi, Removal of ammonium from swine wastewater using synthesized zeolite from Fly ash, Sustainability 12 (2020) 3423, https://doi.org/10.3390/su12083423.
[33] Y. He, L. Zhang, X. An, C. Han, Y. Luo, Microwave assistant rapid synthesis MCM-41-NH2 from fly ash and Cr(VI) removal performance, Environ. Sci. Pollut. Res. 26 (2019) 31463–31477, https://doi.org/10.1007/s11356-019-06255-y.
[34] T. Zheng, X. Zhou, J. Guo, C. Zhong, Y. Liu, Activated mineral adsorbent for the efficient removal of Pb (II) and cd (II) from aqueous solution: adsorption performance and mechanism studies, Water Sci. Technol. 82 (9) (2020) 1896–1911, https://doi.org/10.2166/wst.2020.453.
[35] R. Apiratikul, P. Pavasant, Sorption of Cu^{2+}, Cd^{2+}, and Pb^{2+} using modified zeolite from coal fly ash, Chem. Eng. J. 144 (2008) 245–258, https://doi.org/10.1016/j.cej.2008.01.038.
[36] L. Remenárová, M. Pipíška, E. Florková, M. Horník, M. Rozložník, J. Augustín, Zeolites from coal fly ash as efficient sorbents for cadmium ions, Clean Techn. Environ. Policy 16 (2014) 1551–1564, https://doi.org/10.1007/s10098-014-0728-5.
[37] E. Elkhatib, A. Mahdy, F. Sherif, W. Elshemy, Competitive Adsorption of Cadmium (II) from Aqueous Solutions onto Nanoparticles of Water Treatment Residual, J. Nanomater. (2016), 8496798, https://doi.org/10.1155/2016/8496798.
[38] M. Samiullah, Z. Aslam, A.G. Rana, A. Abbas, W. Ahmad, Alkali-activated boiler fly ash for Ni (II) removal: characterization and parametric study, water, air, Soil Pollut. 229 (4) (2018) 113, https://doi.org/10.1007/s11270-018-3758-5.
[39] A. Alahabadi, P. Singh, P. Raizada, I. Anastopoulos, S. Sivamani, G.L. Dotto, M. Landarani, A. Ivanets, G.Z. Kyzas, A. Hosseini-Bandegharaei, Activated carbon from wood wastes for the removal of uranium and thorium ions through modification with mineral acid, Colloids Surf. A Physicochem. Eng. Asp. 607 (2020) 125516, https://doi.org/10.1016/j.colsurfa.2020.125516.
[40] S.A. Sajjadi, A. Mohammadzadeh, H.N. Tran, I. Anastopoulos, G.L. Dotto, Z.R. Lopičić, S. Sivamani, A. Rahmani-Sani, A. Ivanets, A. Hosseini-Bandegharaei, Efficient mercury removal from wastewater by pistachio wood wastes-derived activated carbon prepared by chemical activation using a novel activating agent, J. Environ. Manag. 223 (2018) 1001–1009, https://doi.org/10.1016/j.jenvman.2018.06.077.
[41] X.B. Li, J.J. Ye, Z.H. Liu, Y.Q. Qiu, L.J. Li, S. Mao, X. Wang, Q. Zhang, Microwave digestion and alkali fusion assisted hydrothermal synthesis of zeolite from coal fly ash for enhanced adsorption of cd (II) in aqueous solution, J. Cent. South Univ. 25 (1) (2018) 9–20, https://doi.org/10.1007/s11771-018-3712-0.
[42] M. Kosmulski, IEP as a parameter characterizing the pH-dependent surface charging of materials other than metal oxides, Adv. Colloid Interf. Sci. 171 (2012) 77–86, https://doi.org/10.1016/j.cis.2012.01.005.
[43] EPA Test Method 1311–TCLP, https://www.epa.gov/sites/production/files/2015-12/documents/1311.pdf.
[44] G. Buema, G. Lisa, O. Kotova, G. Ciobanu, L. Ivaniciuc, L. Favier, M. Harja, Application of thermal analysis to improve the preparation conditions of zeolitic materials from flying ash, Env. Eng.Manag. J. 20 (3) (2021) 377–388.
[45] R.D. Bucur, C. Cimpeanu, M. Barbuta, G. Ciobanu, G. Paraschiv, M. Harja, A comprehensive characterization of ash from Romania thermal power plant, J. Food Agric. Environ. 12 (2) (2014) 943–949.
[46] S.V. Boycheva, D.M. Zgureva, Surface studies of fly ash zeolites via adsorption/desorption isotherms, Bulg. Chem. Commun. Special Issue A (2016) 101–107.
[47] M. Thommes, K. Kaneko, A.V. Neimark, J.P. Olivier, F. Rodriguez-Reinoso, J. Rouquerol, K.S. Sing, Physisorption of gases, with special reference to the evaluation of surface area and pore size distribution (IUPAC technical report), Pure Appl. Chem. 87 (9–10) (2015) 1051–1069, https://doi.org/10.1515/pac-2014-1117.
[48] S. Boycheva, D. Zgureva, H. Lazarova, K. Lazarova, C. Popov, T. Babeva, M. Popova, Processing of high-grade zeolite nanocomposites from solid fuel combustion by-products as critical raw materials substitutes, Manufact. Rev. 7 (2020) 22, https://doi.org/10.1051/mfreview/2020019.
[49] A. Dutta, Y. Diao, R. Jain, E.R. Rene, S. Dutta, Adsorption of cadmium from aqueous solutions onto coffee grounds and wheat straw: equilibrium and kinetic study, J. Environ. Eng. 142 (2016) 1–6, https://doi.org/10.1061/(ASCE)EE.1943-7870.0001015.
[50] N. Kataria, V.K. Garg, Green synthesis of Fe_3O_4 nanoparticles loaded sawdust carbon for cadmium (II) removal from water: regeneration and mechanism, Chemosphere 208 (2018) 818–828, https://doi.org/10.1016/j.chemosphere.2018.06.022.
[51] Y. Tan, X. Yin, C. Wang, H. Sun, A. Ma, G. Zhang, N. Wang, Sorption of cadmium onto Mg-Fe layered double hydroxide (LDH)-kiwi branch biochar, Env. Pollut. Bioavail. 31 (1) (2019) 189–197, https://doi.org/10.1080/26395940.2019.1604165.
[52] X. Huang, H. Zhao, G. Zhang, J. Li, Y. Yang, P. Ji, Potential of removing cd (II) and Pb (II) from contaminated water using a newly modified fly ash, Chemosphere 242 (2020) 125148.
[53] H. Javadian, F. Ghorbani, H.A. Tayebi, S.H. Asl, Study of the adsorption of cd (II) from aqueous solution using zeolite-based geopolymer, synthesized from coal fly ash; kinetic, isotherm and thermodynamic studies, Arab. J. Chem. 8 (6) (2015) 837–849, https://doi.org/10.1016/j.arabjc.2013.02.018.
[54] Y. Taamneh, S. Sharadqah, The removal of heavy metals from aqueous solution using natural Jordanian zeolite, Appl Water Sci 7 (4) (2017) 2021–2028, https://doi.org/10.1007/s13201-016-0382-7.
[55] G. Buema, A.I. Borhan, D.D. Herea, G. Stoian, H. Chiriac, N. Lupu, T. Roman, A. Pui, M. Harja, D. Gherca, Magnetic solid-phase extraction of cadmium ions by self-assembled multicore type Nanobeads, Polymers 13 (2021) 229, https://doi.org/10.3390/polym13020229.
[56] F.A. Olabemiwo, B.S. Tawabini, F. Patel, T.A. Oyehan, M. Khaled, T. Laoui, Cadmium removal from contaminated water using polyelectrolyte-coated industrial waste fly ash, Bioinorg. Chem. Appl. (2017), 7298351, https://doi.org/10.1155/2017/7298351.
[57] K. He, Y. Chen, Z. Tang, Y. Hu, Removal of heavy metal ions from aqueous solution by zeolite synthesized from fly ash, Environ. Sci. Pollut. Res. 23 (2016) 2778–2788, https://doi.org/10.1007/s11356-015-5422-6.
[58] R. Pelalak, Z. Heidari, S.M. Khatami, T.A. Kurniawan, A. Marjani, S. Shirazian, Oak wood ash/GO/Fe_3O_4 adsorption efficiencies for cadmium and lead removal from aqueous solution: kinetics, equilibrium and thermodynamic evaluation, Arab. J. Chem. 14 (3) (2021) 102991, https://doi.org/10.1016/j.arabjc.2021.102991.
[59] S.R. Korake, P.D. Jadhao, Investigation of Taguchi optimization, equilibrium isotherms, and kinetic modeling for cadmium adsorption onto deposited silt, Heliyon 7 (2021), e05755, https://doi.org/10.1016/j.heliyon.2020.e05755.
[60] A. Pholosi, E.B. Naidoo, A.E. Ofomaja, Intraparticle diffusion of Cr (VI) through biomass and magnetite coated biomass: a comparative kinetic and diffusion study, S. Afr. J. Chem. Eng. 32 (2020) 39–55, https://doi.org/10.1016/j.sajce.2020.01.005.
[61] Y.S. Ho, J.F. Porter, G. McKay, Equilibrium isotherm studies for the sorption of divalent metal ions onto peat: copper, nickel and lead single component systems, Water Air Soil Pollut. 141 (2002) 1–33, https://doi.org/10.1023/A:1021304828010.
[62] H. Paudyal, K. Ohto, H. Kawakita, K. Inoue, Recovery of fluoride from water through adsorption using orange-waste gel, followed by desorption using saturated lime water, J. Mater. Cycles Waste Manag. 22 (2020) 1484–1491, https://doi.org/10.1007/s10163-020-01042-1.
[63] V. Jayakumar, S. Govindaradjane, M. Rajasimman, Efficient adsorptive removal of zinc by green marine macro alga Caulerpa scalpelliformis characterization, optimization, modeling, isotherm, kinetic, thermodynamic, desorption and regeneration studies, Surf. Interfaces. 22 (2021) 100798, https://doi.org/10.1016/j.surfin.2020.100798.
[64] M.T. Amin, A.A. Alazba, M. Shafiq, Adsorptive removal of reactive black 5 from wastewater using Bentonite clay: isotherms, kinetics and thermodynamics, Sustainability 7 (2015) 15302–15318, https://doi.org/10.3390/su71115302.
[65] X. Chen, Modeling of experimental adsorption isotherm data, Information 6 (2015) 14–22, https://doi.org/10.3390/info6010014.
[66] T.S. Khayyun, A.H. Mseer, Comparison of the experimental results with the Langmuir and Freundlich models for copper removal on limestone adsorbent, Appl Water Sci 9 (2019) 170, https://doi.org/10.1007/s13201-019-1061-2.
[67] R. Dahake, P. Tiwari, A. Bansiwal, Multicycle adsorption and desorption for recovery of U (VI) from aqueous solution using oxime modified zeolite-a, J. Radioanal. Nucl. Chem. 327 (2021) 133–142, https://doi.org/10.1007/s10967-020-07482-1.
[68] H. Zhao, F. Song, F. Su, Y. Shen, P. Li, Removal of cadmium from contaminated groundwater using a novel silicon/aluminum nanomaterial: An experimental study, Arch. Environ. Contam. Toxicol. 80 (2021) 234–247, https://doi.org/10.1007/s00244-020-00784-1.